

ELM Characterization and Dynamics at Near-Unity A in the Pegasus ST

M.W. Bongard,

J.L. Barr, R.J. Fonck, D.M. Kriete, J.A. Reusch, K.E. Thome



University of
Wisconsin-Madison

26th IAEA Fusion Energy
Conference

Kyoto, Japan
Presentation EX/P4-51
October 19, 2016



PEGASUS
Toroidal Experiment

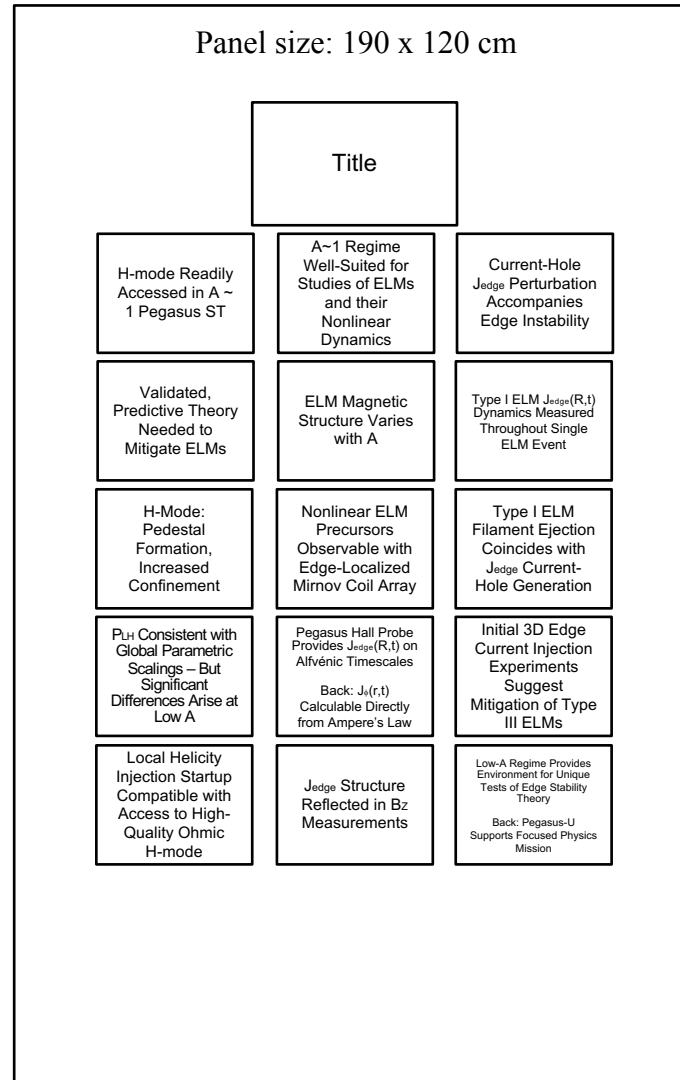


Poster Layout

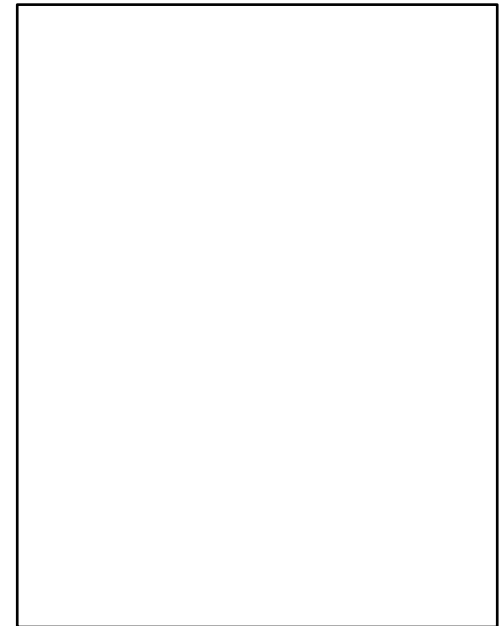
10:1 scale

US Legal
8.5 x 14"

US Letter
8.5 x 11"



Recommended layout: 110 x 85 cm



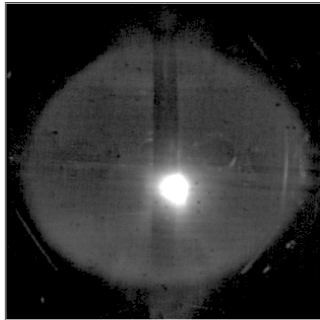


H-mode Readily Accessed in A ~ 1 PEGASUS ST

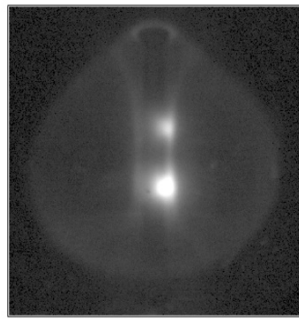
Limited L



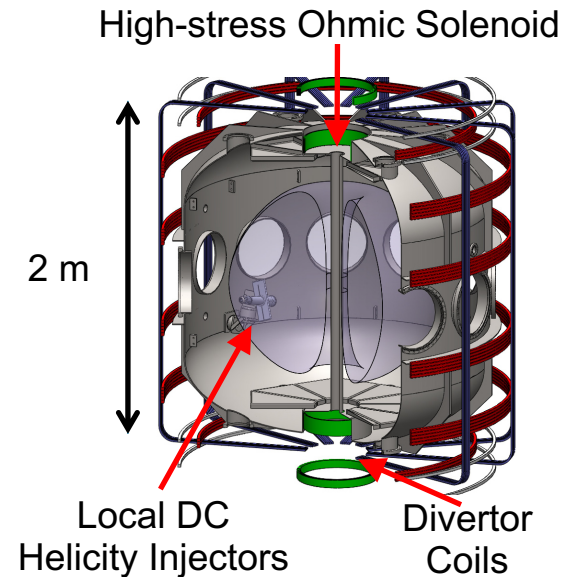
Limited H



Diverted H



Fast visible imaging, $\Delta t \sim 30 \mu s$



- Low B_T at $A \sim 1 \rightarrow$ low H-mode P_{LH}

- $P_{OH} \gg P_{ITPA08} \sim B_T^{0.80} n_e^{0.72} S^{0.94}$
- Limited or diverted topology
- Facilitated by HFS fueling

- Standard H-mode features observed

- Unique edge diagnostic access

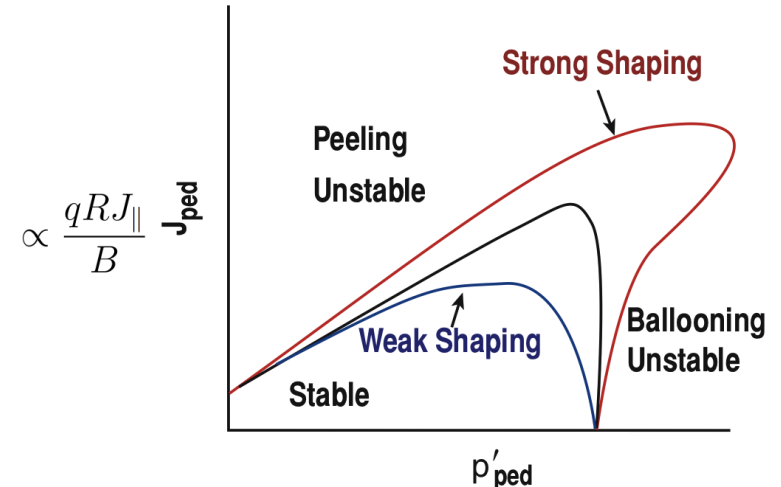
PEGASUS Toroidal Experiment

A	1.15 – 1.3
R (m)	0.2 – 0.45
I_p (MA)	≤ 0.25
B_T (T)	< 0.2
$\Delta\tau_{shot}$ (s)	≤ 0.025
Wall Type	SS + Ti getter

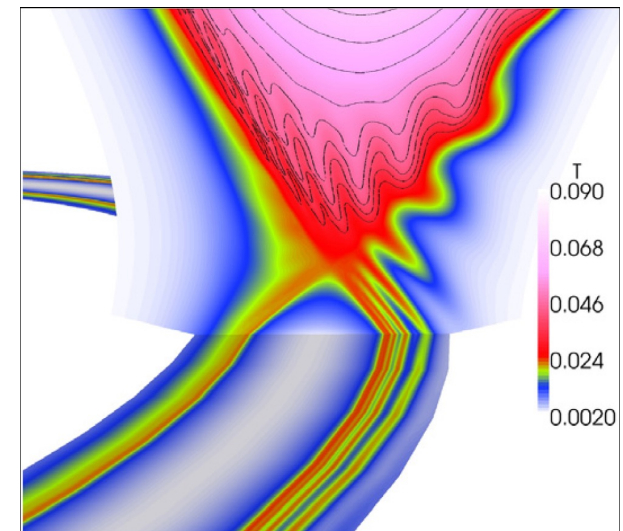


Validated, Predictive Theory Needed to Mitigate ELMs

- Peeling-ballooning model
 - Competing ideal MHD instabilities cause ELM onset
 - Current-driven peeling modes
 - Pressure-driven ballooning modes
- Nonlinear extensions
 - More complete physical models
 - Evolution of P-B mode structures
 - Heat flux deposition projections
- Detailed measurements required to validate theory
 - $P_{\text{edge}}, J_{\text{edge}}(R,t)$ on ELM timescales



Snyder et al., *Phys. Plasmas* 12, 056115 (2005)
Hegna, *Phys. Plasmas* 3, 584 (1996)

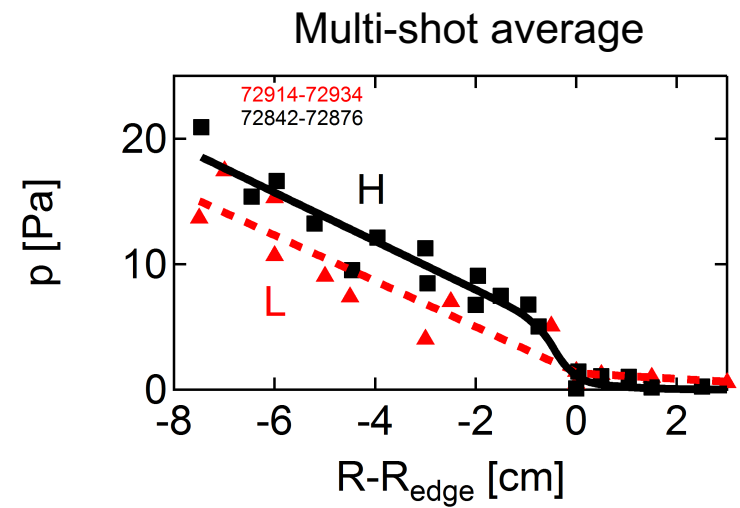
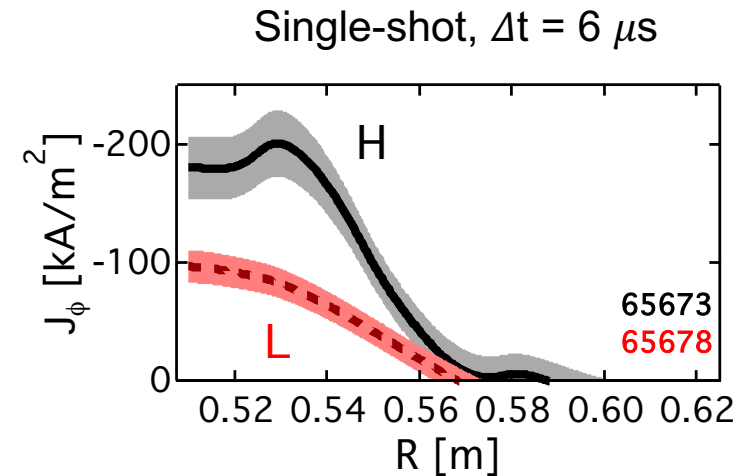


Huysmans et al., *Plasma Phys. Control. Fusion* 51, 124012 (2009)



H-mode: Pedestal Formation, Increased Confinement

- Short pulse, low $T_{e,edge}$
- **Simple probe access across pedestal**
- J_ϕ , P pedestals in H-phase
 - $J_\phi(R,t)$: multichannel Hall probe
 - $p(R)$: triple Langmuir probe
- Confinement increases 2x
 - Requires time-evolving reconstructions
 - L: $H_{98} \sim 0.5 \pm 0.2$
 - H: $H_{98} \sim 1.0 \pm 0.2$

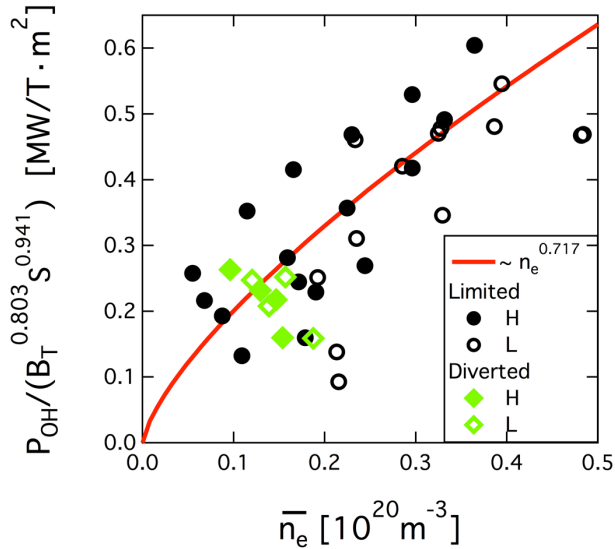


Bongard et al., *Rev. Sci. Instrum.* **81**, 10E105 (2010)
Bongard et al., *Phys. Rev. Lett.* **107**, 035003 (2011)
Thome et al., *Phys. Rev. Lett.* **116**, 175001 (2016)
Thome et al., *Nucl. Fusion* **57**, 022018 (2017)

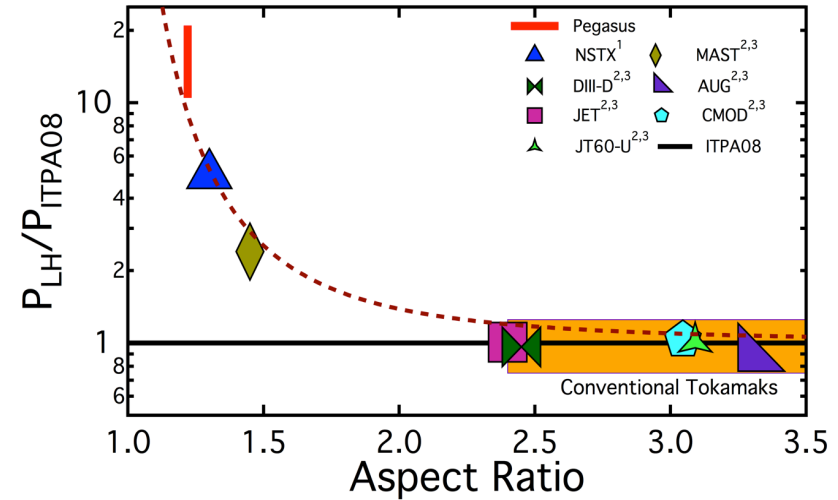


P_{LH} Consistent with Global Parametric Scalings— But Significant Differences Arise at Low A

Normalized P_{LH} vs. Density



Normalized P_{LH} vs. Aspect Ratio

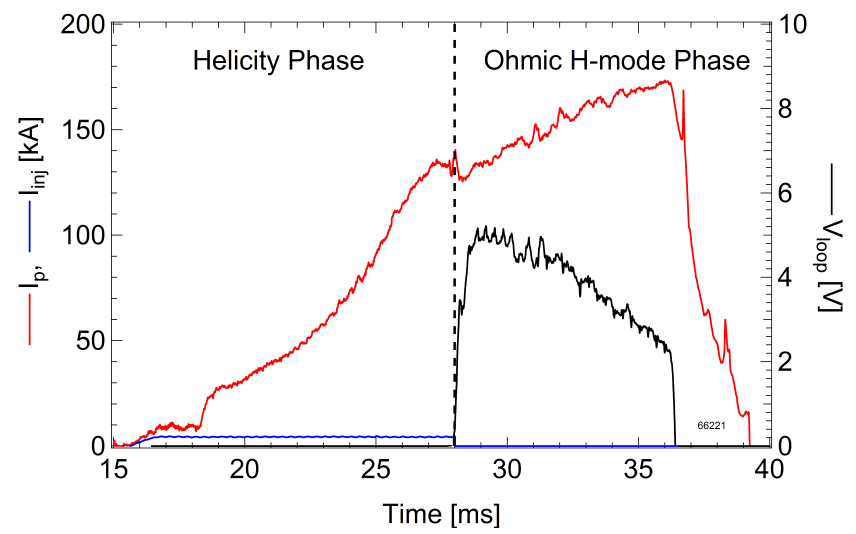
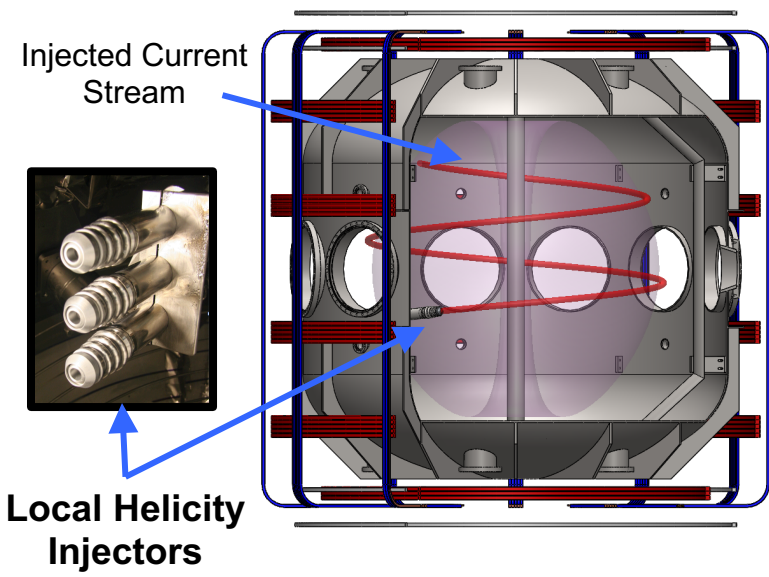


- $P_{LH}(n_e)$ follows ITPA scaling
 - FM³ model: minimum $P_{LH}(n_e) \sim 1 \times 10^{18} \text{ m}^{-3}$
- Magnetic topology independence
 - Diverted, limited edge topology similar
 - FM³: $P_{LH}^{LIM} / P_{LH}^{DIV} \sim (q_*^{LIM} / q_*^{DIV})^{-7/9}$

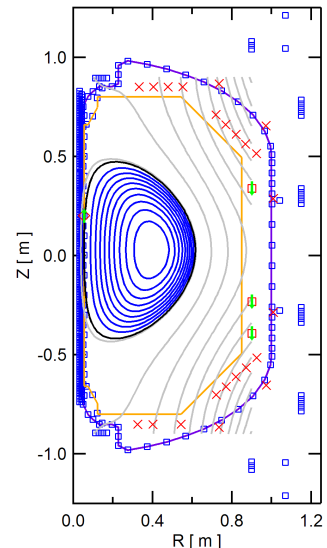
- At low A, $P_{LH} \gg P_{ITPA08}$
 - P_{LH} increasingly diverges from expectations as $A \rightarrow 1$
 - $P_{LH} / P_{ITPA08} \sim 15$ at $A \sim 1.2$



Local Helicity Injection Startup Compatible with Access to High-Quality Ohmic H-mode



- High- I_p , long-pulse H-mode plasmas desirable
 - Confinement, edge stability studies; attaining high β_T
- LHI creates tokamak plasmas via edge current drive
 - Taylor relaxation, helicity balance
- No fundamental obstacles to H-mode access from LHI physics



Equilibrium Parameters
Shot 66221, 34.80 ms

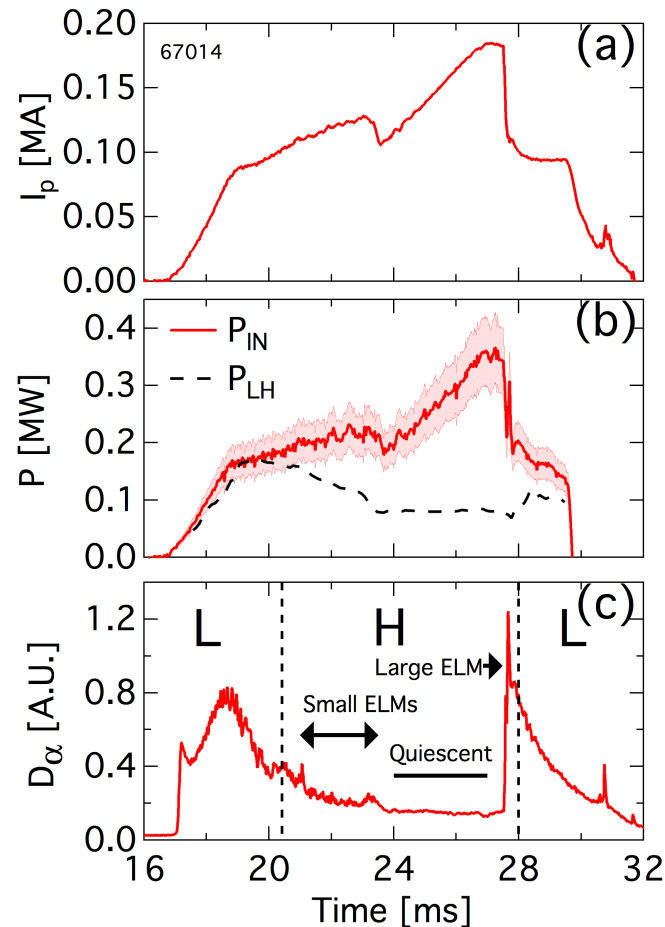
I_p	169 kA	R_0	0.336 m
β_t	0.081	a	0.281 m
l_i	0.42	A	1.20
β_p	0.31	κ	1.6
W	2101 J	δ	0.44
B_{T0}	0.179 T	q_{95}	9.92



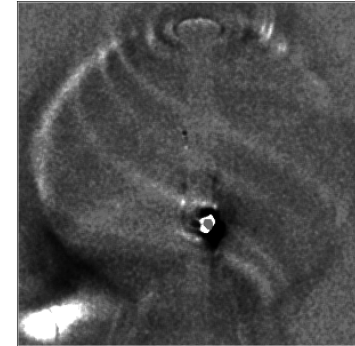
A ~ 1 Regime Well-Suited for Studies of ELMs and their Nonlinear Dynamics

- ELMs create 3D filaments
 - Coincident with D_α bursts
- Small (“Type III”):
 - Low-n, peeling-like
 - Observed at $P_{OH} \sim P_{LH}$
- Large (“Type I”)
 - Intermediate n
 - Observed at $P_{OH} \gg P_{LH}$

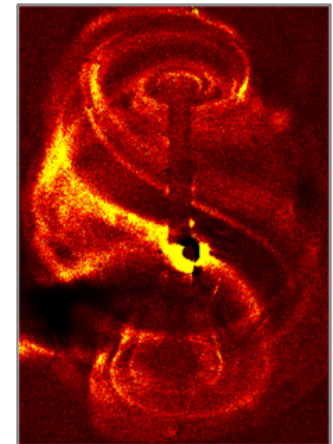
Evolution of Discharge with Small, Large ELMs with P_{OH} ramp



Small (Type III) ELM



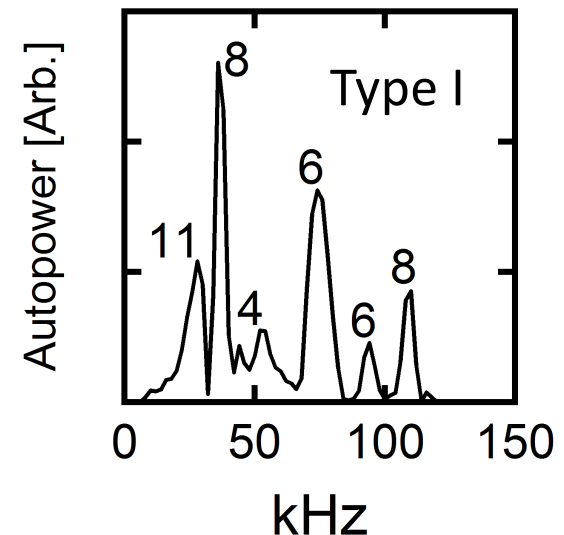
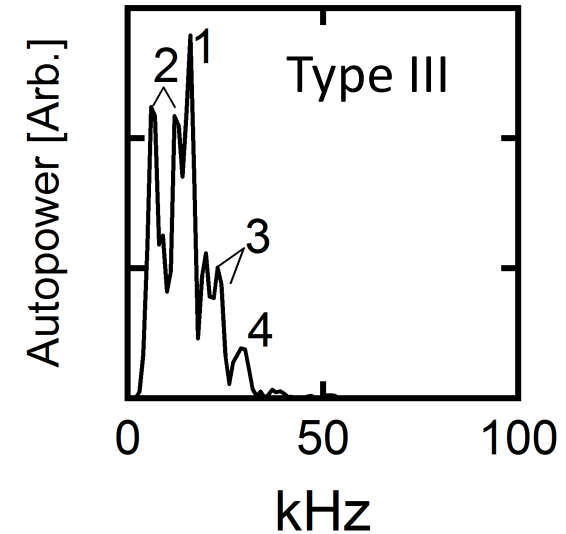
Large (Type I) ELM





ELM Magnetic Structure Varies with A

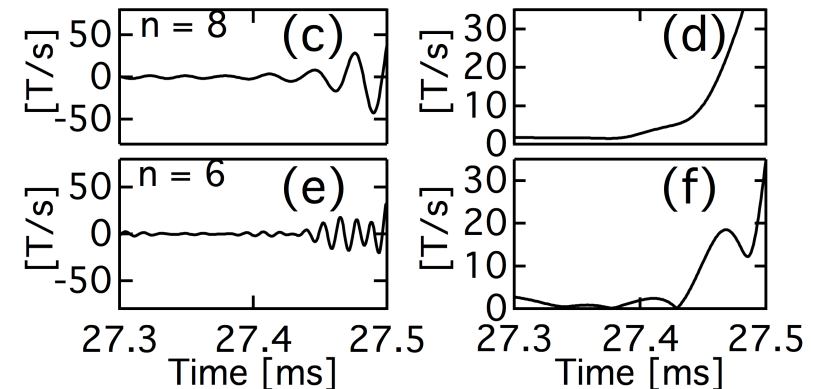
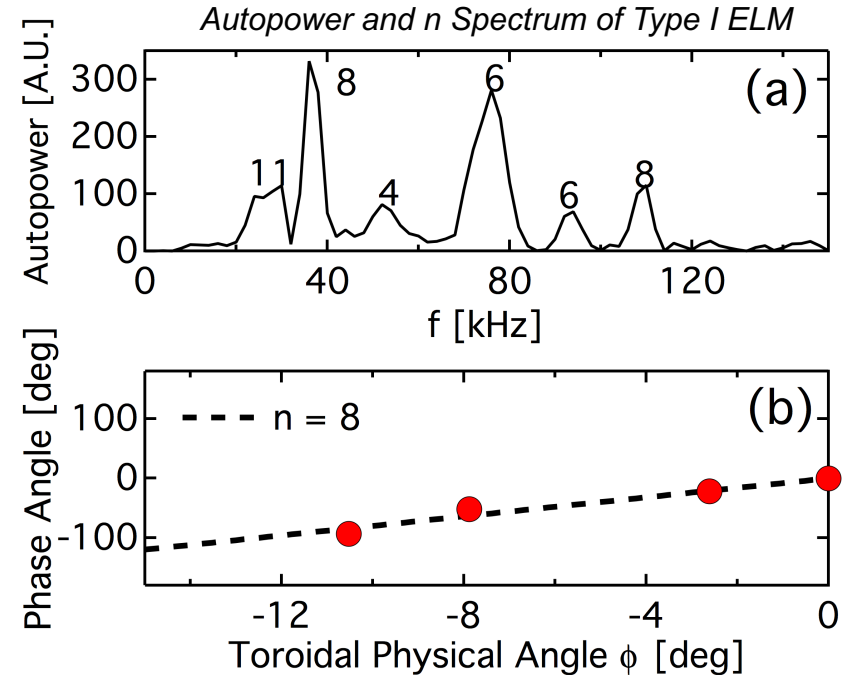
- Edge Mirnov array measures ELM toroidal mode spectrum
 - $n \leq 20$ resolved by multipoint cross-phase analyses
- Type III: A dependent
 - Low $A \leq 1.4$: $n \leq 1 - 4$
 - PEGASUS, NSTX
 - Conventional $A \sim 3$: $n > 8$
- Type I: A independent
 - Intermediate- n
 - Low- A devices have lower n
- Increased peeling drive at low- A
 - Higher $J_{\text{edge}}/B \rightarrow$ lower n





Nonlinear ELM Precursors Observable with Edge-Localized Mirnov Coil Array

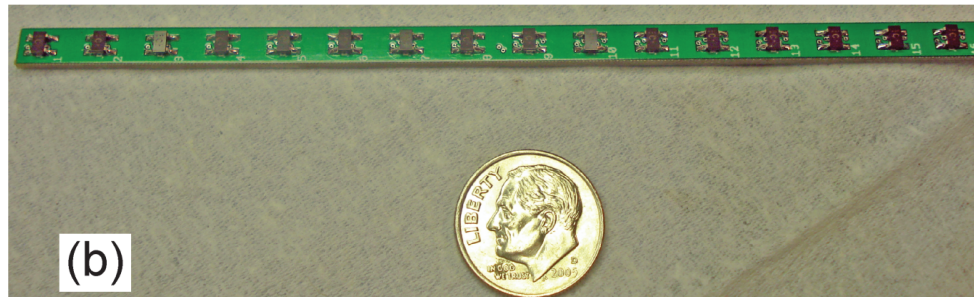
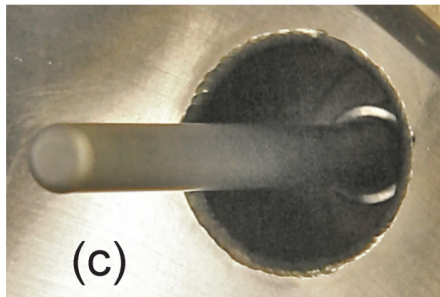
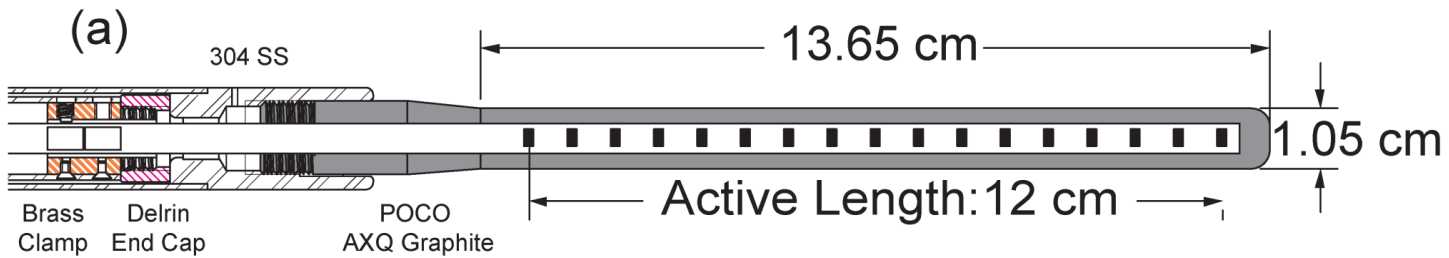
Fast Visible Imaging Across Type I ELM



- Simultaneously unstable n during ELM
 - Detectable only within \sim cm of LCFS
 - Nonlinear energy exchange
- Modes grow on MHD timescales
 - $n = 8$ grows continuously
 - $n = 6$ fluctuates prior to crash



PEGASUS Hall Probe Provides $J_{\text{edge}}(R, t)$ on Alfvénic Timescales



Bongard et al., *Rev. Sci. Instrum.* **81**, 10E105 (2010)

- Precision $B_z(R, t)$ measurements
 - 16 solid-state InSb Hall sensors
 - 7.5 mm radial resolution
 - 75 kHz large-signal bandwidth
 - 175 kHz small-signal bandwidth
- J_ϕ obtained directly via Ampère's Law
 - Assumes local tokamak equilibrium
 - No profile parameterization constraint
- Carbon Armored
 - Compatible with L, H-mode to date

$$\mu_0 J_\phi = -\frac{B_z}{\kappa^2 (R - R_0)} \left(1 - \frac{Z^2 R_0}{\kappa^2 R (R - R_0)^2} \right) - \frac{dB_z}{dR} \left(1 + \frac{Z^2}{\kappa^4 (R - R_0)^2} \right)$$



$J_\phi(R,t)$ Calculable Directly from Ampère's Law

$$\mu_0 J_\phi = (\nabla \times \mathbf{B})_\phi = \frac{\partial B_R}{\partial Z} - \frac{\partial B_Z}{\partial R}$$

- Simplest test follows from $B_R(Z)$ or $B_Z(R)$ measurements
- Petty solves for an off-midplane $B_Z(R)$ measurement set and an elliptical plasma cross-section:

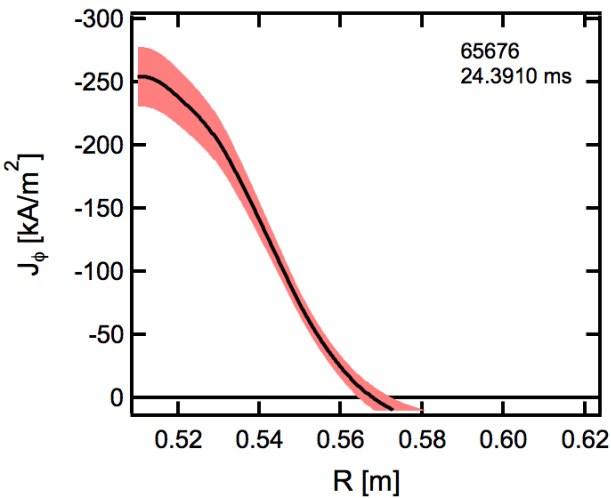
$$\mu_0 J_\phi = -\frac{B_Z}{\kappa^2 (R - R_0)} \left(1 - \frac{Z^2 R_0}{\kappa^2 R (R - R_0)^2} \right) - \frac{dB_Z}{dR} \left(1 + \frac{Z^2}{\kappa^4 (R - R_0)^2} \right)$$

- Does not make assumptions on shape of $J(R)$

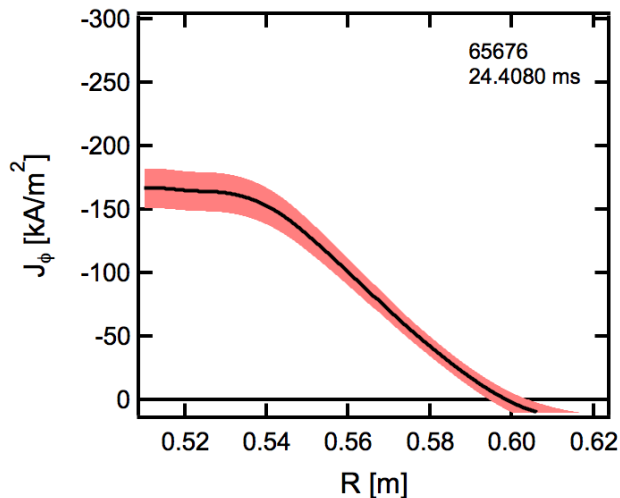


J_{edge} Structure Reflected in B_z Measurements

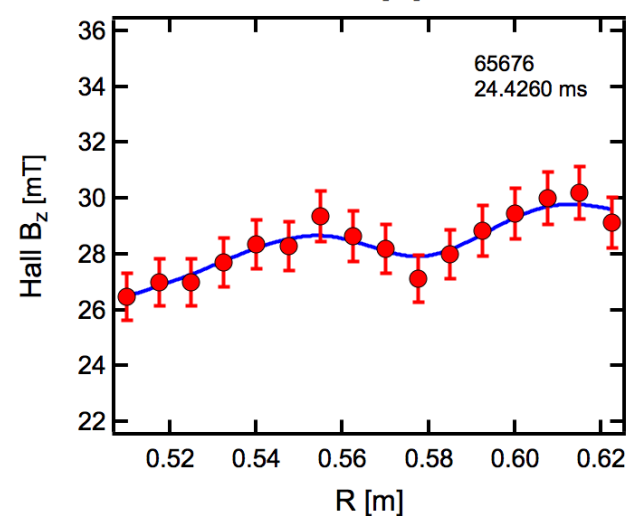
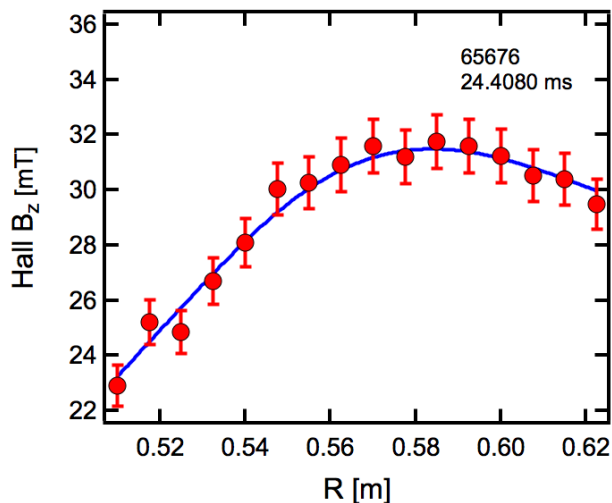
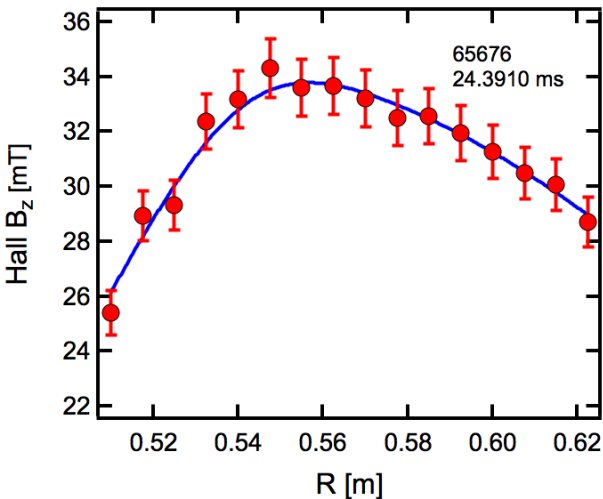
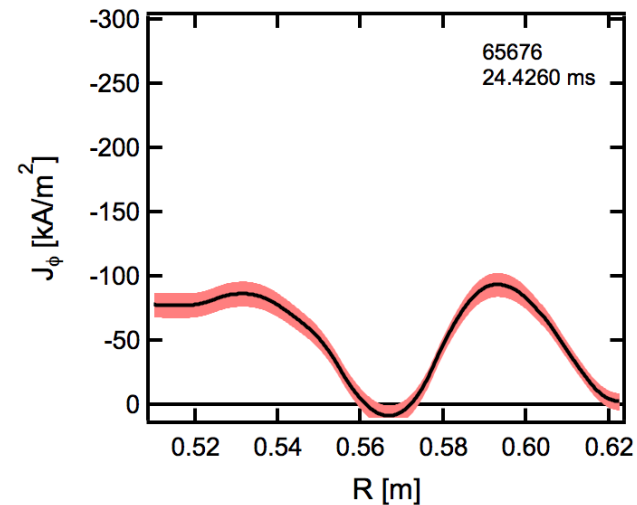
Type I Peak



Type I Mid-Crash

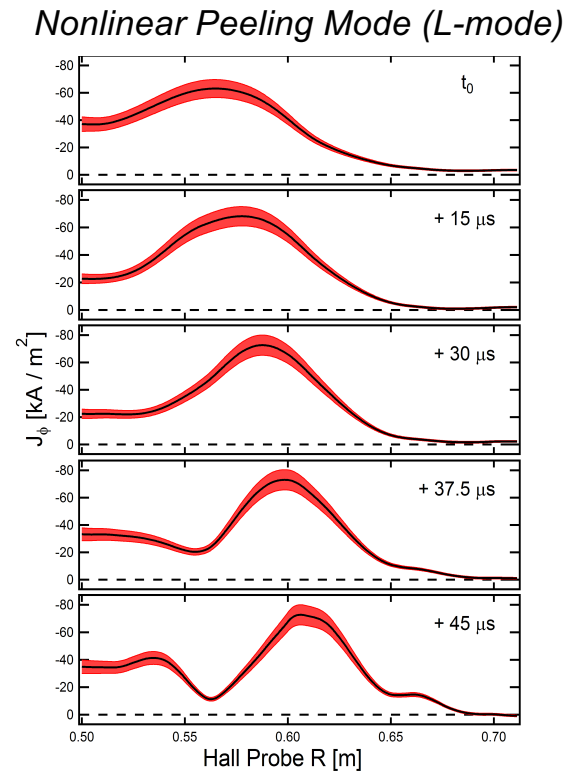
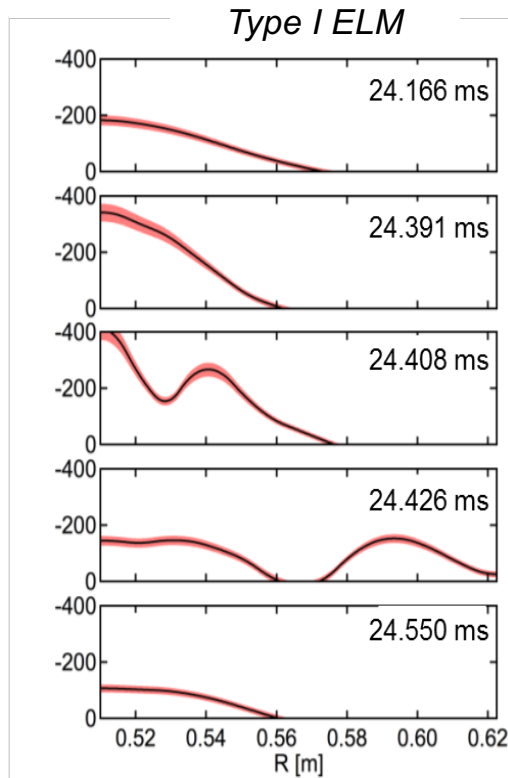
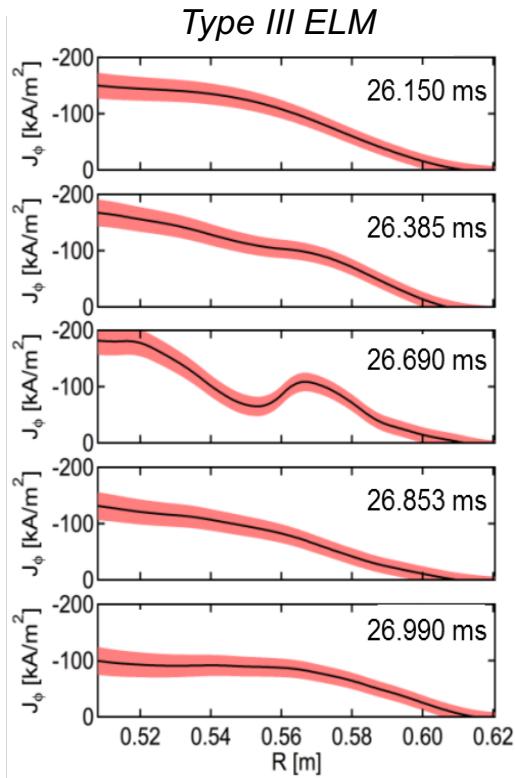


Filament Expulsion





Current-Hole J_{edge} Perturbation Accompanies Edge Instability

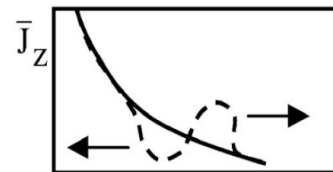
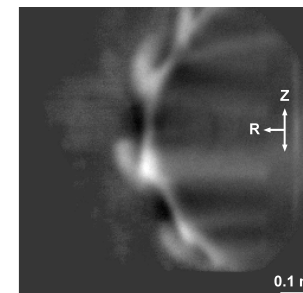


Feature observed during ELMs and peeling modes

- Validates mechanism hypothesized by EM blob transport theory
- Type III ELM: smaller perturbation, slower, no filament evident
- Type I: larger, faster, filament expulsion

Nonlinear Peeling Mode Filaments

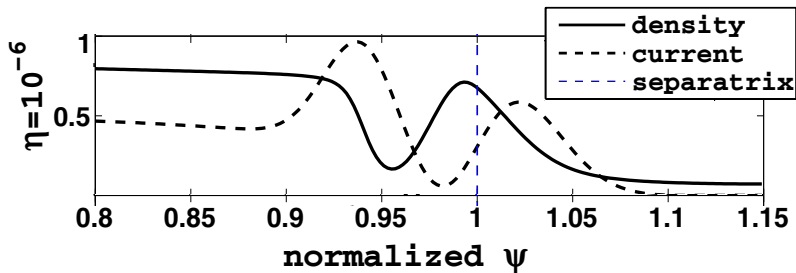
Model of "Current-Hole" Filament Ejection





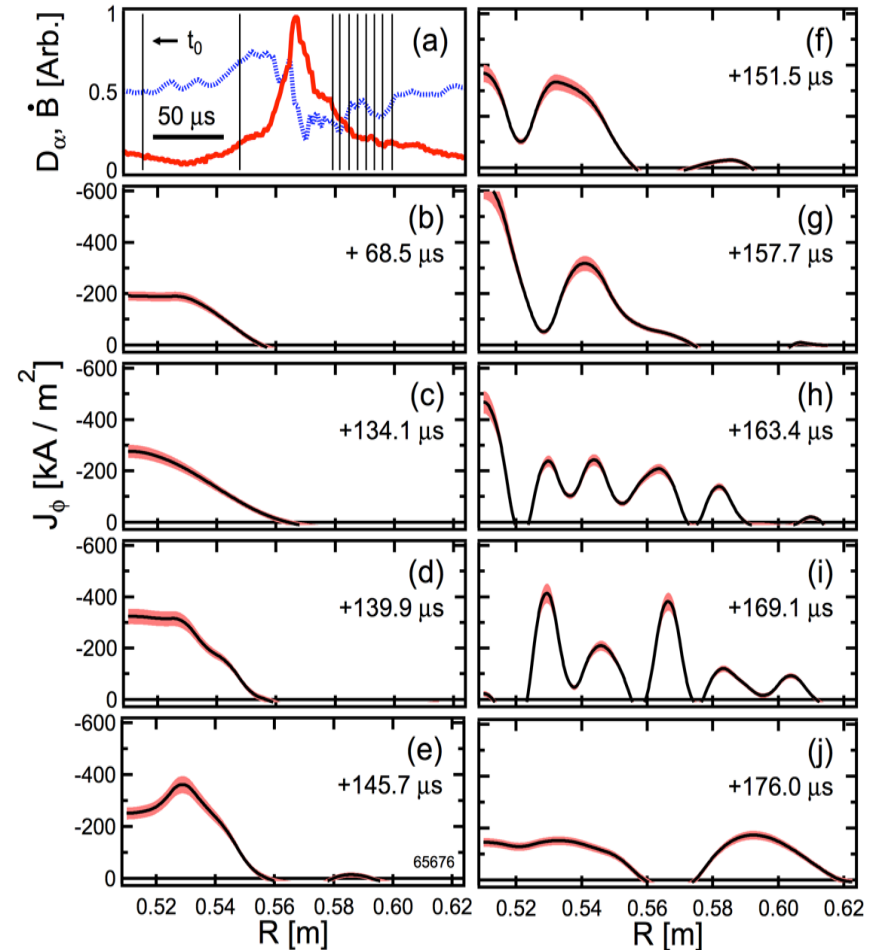
Type I ELM $J_{\text{edge}}(R,t)$ Dynamics Measured Throughout Single ELM Event

- **Challenge:** nonlinear ELM dynamics at Alfvénic timescales
- Current profile evolution through ELM cycle shows complex multimodal behavior
 - Less spatial smoothing employed in Hall probe analysis
- Opportunities for detailed comparison to nonlinear MHD simulations
 - e.g. NIMROD, JOEK, BOUT++



Pamela et al., *Plasma Phys. Control. Fusion* 53, 054014 (2011)

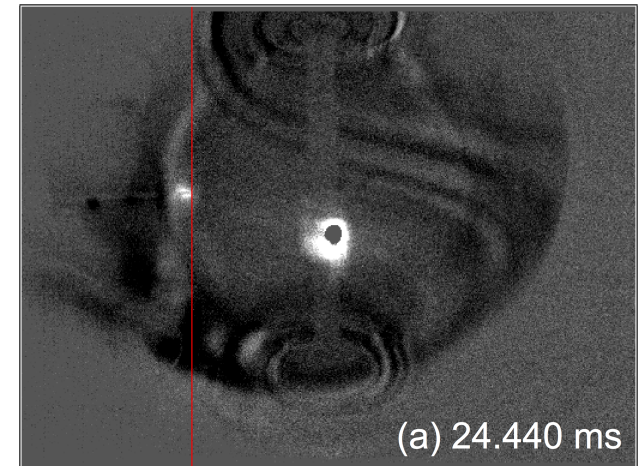
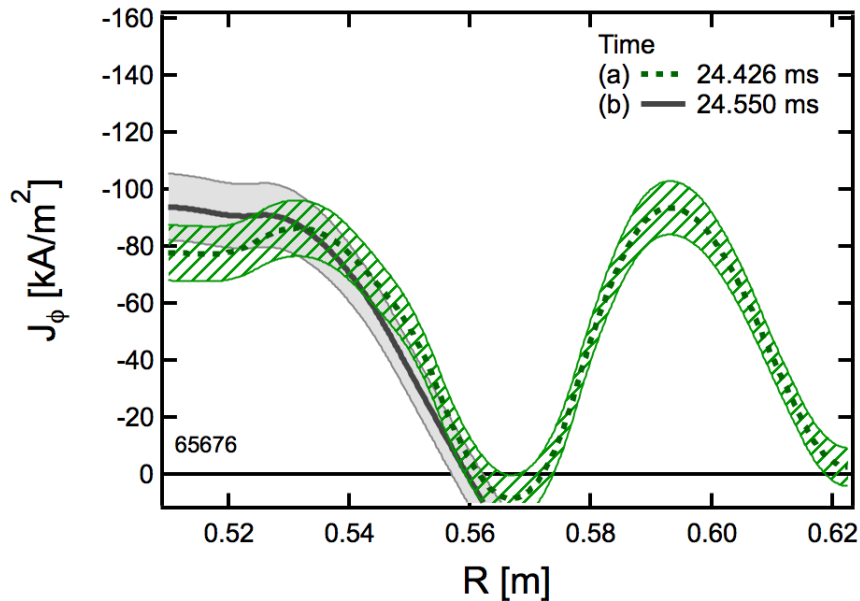
Type I ELM Evolution



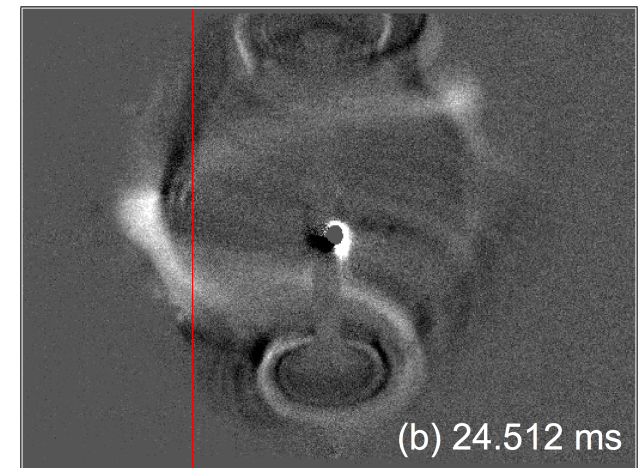
Thome et al., *Phys. Rev. Lett.* 116, 175001 (2016)



Type I ELM Filament Ejection Coincides with J_{edge} Current-Hole Generation



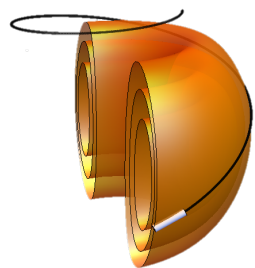
Nearest Imaging Times; Prior Frame Subtracted



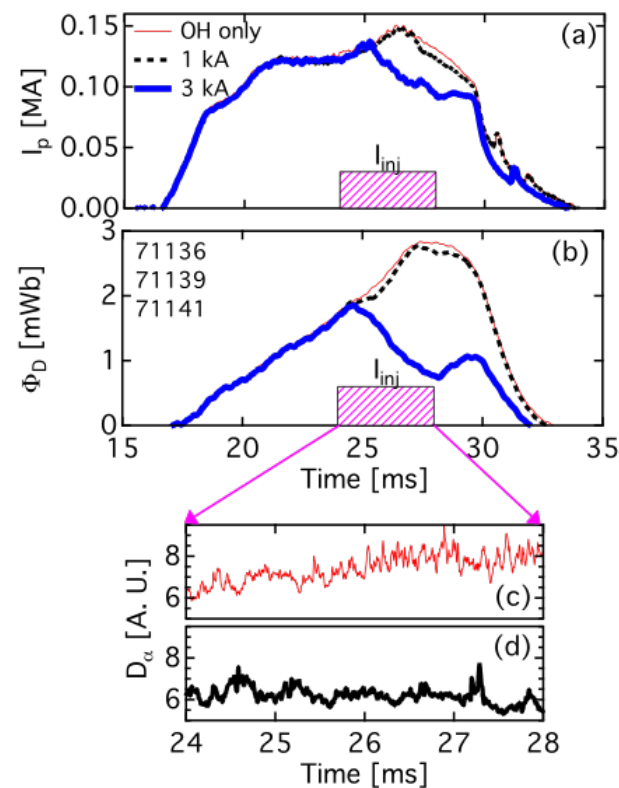
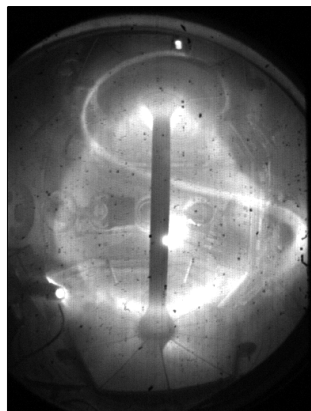
- Outwardly-propagating filament observed with high-speed visible imaging in ELM crash



Initial 3D Edge Current Injection Experiments Suggest Mitigation of Type III ELMs



- Local helicity injection system provides 3D SOL current injection
 - $I_{inj} \leq 5$ kA, $J_{inj} \sim 1$ kA/cm²
 - Strong 3D edge current perturbation
 - Similar to LHCD on EAST
 - Edge biasing: modify rotation
- Low levels of J_{edge} injection into H-mode reduce ELM activity
 - Low I_{inj} = ELM suppression
 - High I_{inj} = edge, shot degradation





Low-A Regime Provides Environment for Unique Tests of Edge Stability Theory

H-mode Physics with Pedestal Diagnostic Access

- Standard features: J, p pedestals; low D_α , increased τ_e
- Features unique to low-A emerging: P_{LH} threshold

ELM Regimes Identified with Differing n Spectra

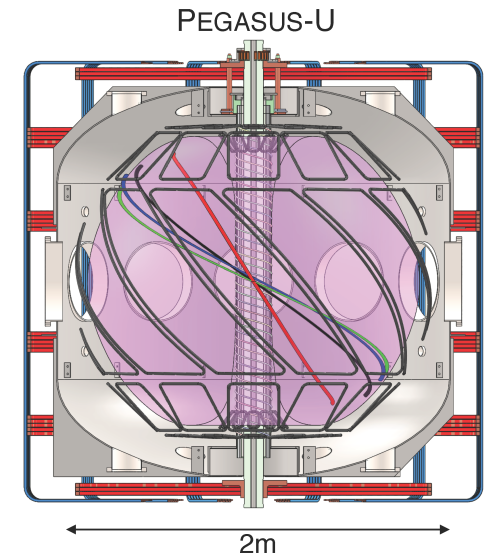
- Large, Type I-like: intermediate n
- Small, Type III-like: low n
- Simultaneous spectrum of n present during crash

Nonlinear ELM Dynamics on Alfvénic Timescales

- Nonlinear energy exchange in n modes prior to crash
- Fast $J_{edge}(R, t)$: current-hole perturbation, filament expulsion

Helical Edge Current Injection Affects Type III ELMs

- Potential dual use of LHI injectors as ELM control actuator



Proposed Upgrades:

- Pedestal physics, nonlinear ELM physics and mitigation
- Local Helicity Injection in NSTX-U relevant conditions



PEGASUS-U Supports Focused Physics Mission

- Nonlinear pedestal and ELM studies
 - Simultaneous measurements of $p(R,t)$, $J(R,t)$, $v_\phi(R,t)$
 - New edge diagnostics (probe arrays, DNB)
 - Tests of Sauter neoclassical bootstrap model
- ELM Modification and Mitigation
 - Novel 3D-MP coil array
 - LFS array: 12 toroidal \times 7 poloidal
 - Helically-wound HFS coils
 - LHI current injectors in divertor, LFS regions
- Physics of Local Helicity Injection Startup
 - High I_p , long-pulse startup
 - Projections to NSTX-U

